

Growth and Characterization of $\text{Bi}_{2+x}\text{Sr}_{2-x}\text{CuO}_{6+\delta}$ Single Crystals

Huiqian Luo, Lei Fang, Gang Mu, Hai-Hu Wen

National Laboratory for Superconductivity, Institute of Physics and
National Laboratory for Condensed Matter Physics, P. O. Box 603 Beijing, 100080, P. R. China

Abstract

High-quality $\text{Bi}_{2+x}\text{Sr}_{2-x}\text{CuO}_{6+\delta}$ ($0 < x \leq 0.5$) single crystals have been grown successfully using the travelling-solvent floating-zone(TSFZ) technique. The samples with $x \geq 0.05$ are in the underdoped level with an upturn of resistivity in low temperature region. The crystal structure of these samples was investigated by X-Ray diffraction. The evolution of c-axis lattice parameters with varied x is displayed, which is strongly associated with the behavior of T_c . The crystals exhibit superconducting transitions with $T_c = 9$ to 1 K for the samples with $x = 0.05$ to 0.20, while for samples with $x = 0.25$ and above no superconductivity was discovered down to 1.6 K. The resistivity of samples with $x = 0.31, 0.40$ and 0.50 exhibits a drastic divergence as temperature approaches 0 K, which suggests a strong localization effect induced by the out-of-plane disorders.

Key words: A2. Travelling solvent zone growth, B2. Oxide superconducting materials, B1. Cuprates, B1. Bismuth compounds.
PACS: 74.72.Hs, 74.62.Bf, 74.62.Dh

1. Introduction

Since the high temperature superconductors(HTSCs) were discovered, there has been no consensus yet on the mechanism of the high T_c superconductivity in these materials. Because of the complex structure and anomalous behavior in both superconducting and normal states, it is tempting to conclude that the Landau-Fermi liquid and BCS theories seem inapplicable to describe the physics in the normal and superconducting states. The single-layer copper-oxide superconductor $\text{Bi}_{2+x}\text{Sr}_{2-x}\text{CuO}_{6+\delta}$ (BSCO) is an ideal material for the research of mechanism of HTSC. This system has rather low $T_c \leq 10$ K and a structure with Cu-O conducting layer and carrier reservoir which is similar to other cuprates [1,2,3,4,5,6,7,8,9,10]. A big advantage to conduct investigation on this system is that the upper critical field is rather low and the superconductivity can be easily suppressed by applying a magnetic field [11,12,13], so both of the superconductivity and normal state characteristics can be easily investigated. In addition, the nature of the ground state of pseudogap is still highly debated [14], this system may provide a possible way to reach the ground state of the pseudogap phase[15]. Comparing to its brother system, the La-doped $\text{Bi}_2\text{Sr}_{2-x}\text{La}_x\text{CuO}_{6+\delta}$ (BSLCO) with identical structure but much higher T_c ($T_{max} \approx 38$ K), the low T_c of the present system was attributed to a greater out-of-plane disorder effect induced

by a larger mismatch of the ionic radius between Sr^{2+} and Bi^{3+} than Sr^{2+} and La^{3+} [16,17,18], but more experiments on good quality single crystals are required to clarify this point.

It was reported that the Bi-based Bi-2201 single crystal could be grown by the self-flux and KCl-solution-melt method[1,2,3,4,5,6,7]. However, large size crystals with high homogeneity and less contamination were still hard to obtain. On the other hand, the optical travelling-solvent floating-zone(TSFZ) method could overcome these drawbacks. As far as we know, only Lin *et. al.* have successfully grown the La-free bulk superconducting $\text{Bi}_{2+x}\text{Sr}_{2-x}\text{CuO}_{6+\delta}$ crystals from the non-stoichiometric starting composition of $\text{Bi}_{2.2}\text{Sr}_{1.9}\text{Cu}_{1.2}\text{O}_{6+\delta}$ and $\text{Bi}_{2.35}\text{Sr}_{1.98}\text{Cu}_{1.0}\text{O}_{6+\delta}$ by TSFZ method under oxygen pressure (≥ 2 bar) [8,9,10]. In this paper, we report the successful growth of large size $\text{Bi}_{2+x}\text{Sr}_{2-x}\text{CuO}_{6+\delta}$ single crystals with high quality by TSFZ method. The x value in the starting composition is varied from 0 to 0.50. The crystals cleaved from the ingots with $x = 0.04 \sim 0.20$ exhibit superconductivity, it seems that the optimal doping point is at the nominal value of $x = 0.05$. Superconductivity has not been observed at $x = 0.25$ and above, and a much stronger low temperature up-turn of resistivity has been observed as x is beyond 0.25. A strong correlation between c -axis parameter and T_c is found suggesting an influential effect on superconductivity by the subtle change of structure.

2. Experiment and Characterization

Before crystal growth, a feed rod with high density is prepared. The polycrystalline material was prepared by an ordinary solid reaction method. Powders of Bi_2O_3 (99.99 %), SrCO_3 (99.99%) and CuO (99.5%) in the target proportion were mixed in an agate mortar for about 4 hours and pressed into cylindrical rods of $\phi 7 \times 85$ mm under hydrostatical pressure with ~ 70 MPa, then calcined in a vertical molisili furnace at 780°C for 36 hours. The rods were crushed into powder to be ground again. This procedure was repeated for 4 times to ensure the homogeneity of the polycrystalline powder. At the last time, the feed rod was sintered at 850°C for more than 36h in order to get a higher density. No crucible was used throughout the whole process, so there was little contamination for the rods. In order to get higher density feed rod with sufficient oxygen content, the premelting was performed under oxygen pressure $P(O_2) = 2$ atm, and the moving speed of mirror stage was $25\sim 30$ mm/hr depending on x values. After premelting, a homogeneous feed rod with $\phi 6$ mm in diameter and $60\sim 90$ mm in length was obtained .

Single crystal growth by the TSFZ method was performed at an optical floating-zone furnace equipped with four ellipsoidal mirrors which was produced by the *Crystal Systems Corporation*. A steep temperature gradient was obtained by using four 300W halogen lamp as the heating source. The crystal growth was under an oxygen pressure in an enclosed quartz tube, two conditions of oxygen pressure $P(O_2)=2$ atm and 6 atm were applied, and the O_2 flowing rate was about $20\sim 40$ cc/min. The growth rate is about 0.50 mm/hr, which sometimes is as slow as 0.40mm/hr or as fast as to 0.60mm/hr in order to obtain a more stable floating-zone and larger crystals. The rotation rate is $25.0\sim 28.0$ rpm for the upper shaft and $14.0\sim 17.0$ rpm for the lower shaft in opposite directions.

In order to check the quality of crystals, the as-grown ingots were cleaved into many pieces of crystals. Then the single crystals selected under microscope were characterized by various techniques. The energy dispersive X-ray (EDX) analysis was used to determine the composition of the crystals. While the X-ray diffraction(XRD) of the crystals was measured to see the crystalline quality of the samples. K_α radiation of Cu target was used, and the continuous scanning range of 2θ is from 5° to 80° . The splitting peaks at high degree angle indicated different wavelength effects between $K_{\alpha 1}$ and $K_{\alpha 2}$ radiation. Before crystal growth, XRD for the powder of polycrystal was also carried out to check the phase purity of starting materials. The c-axis lattice parameters were calculated from XRD patterns of the single crystals. The superconductivity of the crystals was measured with AC susceptibility and resistivity based on an *Oxford* cryogenic system Maglab-EXA-12 and a *Quantum Design* Physical Property Measurement System(PPMS). An alternating magnetic field with $H = 1$ Oe and frequency $f=333$ Hz was applied perpendicular to the ab -plane when

the AC susceptibility measurement was undertaken with the zero-field-cooling(ZFC) method. The transition temperature (T_c) of the crystals was derived from AC susceptibility curve by the point where the real part of the susceptibility becomes flat. A four-probe Ohmic contact with low-resistances ($< 10\Omega$) on ab -plane was used for the resistivity measurement , and the sweeping rate of temperature is about 2K/min from 2K to 300K.

3. Results and discussion

3.1. Crystal growth

The crystal growth was performed under oxygen atmosphere enclosed by quartz tube. At the initial stage of the heating, both the feed rod and seed rod were set apart by a distance of a few mm, the lamp power was increased gradually until both ends of the feed rod and seed rod began to melt. Then the upper feed rod was moved downwards carefully until it touched the seed rod and formed the molten zone. The length and width of floating-zone were adjusted so that its diameter was almost the same as that of the feed and seed rod(about 6 mm).

In order to get high quality single crystal, a stable floating-zone with proper volume should be sustained during the growth. The parameters such as the power of lamp, growth rate, rotation rate of shafts, pressure and flowing rate of oxygen should be carefully chosen. The volume of floating-zone could also be adjusted carefully by the downwards or upwards slow moving of the upper shaft. The length of floating-zone, namely the distance between the feed rod and seed rod, was sensitive to the power of lamps and thus a proper power of lamp was applied. It could be changed $0.1\%\sim 0.5\%$ to get the optimal length of floating-zone. This was suitable for the width of floating-zone which was sensitive to the moving speed of mirror stage, namely, the growth rate of crystal. Sometimes it was tuned to ($< \pm 0.1$ mm/hr) in order to obtain a more stable floating-zone and larger crystals. At the same time, both the upper and lower shafts were rotated in opposite directions, the rotation rates which determine the convex shape of solid-liquid interface could also be changed at a suitable range until the floating-zone was stable enough. Generally, the rotation rate of upper shaft was relatively faster to mix the liquid homogeneously, but the lower shaft was rotated at a lower rate to get a stable floating-zone and large size crystals. Furthermore, the pressure of oxygen could influence on the melting point of the feed rod and stability of floating-zone. Comparing the case between $P(O_2) = 2$ atm and $P(O_2) = 6$ atm, there were no distinct effects on crystal structure and T_c were observed. However, larger flowing rate would lead to larger crystals but make the floating-zone more unstable, while higher pressure did not lead to larger thickness along c-axis of the crystals. This is slightly different from the previous reports.[9,10]

It is noteworthy that all growth parameters depend on

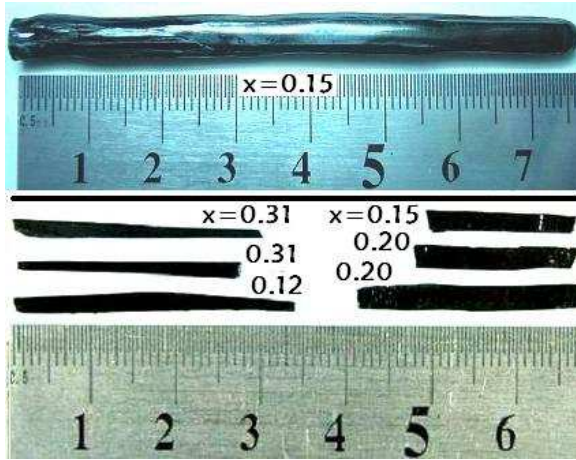


Fig. 1. (color online) As-grown ingot of BSCO with $x=0.15$ (above) and single crystals cleaved from as-grown ingots with $x=0.12$, 0.15 , 0.20 and 0.31 (below).

starting compositions with different x values, because the relative content of Bi_2O_3 influences the melting point of feed rod and the viscosity of the mixed liquid. For $x \geq 0.10$, larger plate-like single crystal could be obtained easily, but for $0 < x < 0.10$, the crystals became smaller and for $x = 0$ there were only tiny needle-like crystals were obtained. In addition, for the too much higher and lower viscosity of compound with $x = 0.50$ and $x = -0.20$ (where Sr was more sufficient than Bi), the floating-zone collapsed frequently and the crystal growth was interrupted. On the other hand, most of as-grown single crystals were in under-doped level, it could be attributed to the deficiency of oxygen content because we did not sinter the feed rod in flowing oxygen but only premelt the feed rod under oxygen pressure $P(\text{O}_2)=2$ atm. One of the as-grown ingots with $x=0.15$ and several as-grown crystals with $x=0.12$, 0.15 , 0.20 and 0.31 are showed in Fig.1. The crystals are sizeable and flat in large area which exhibit the high quality.

3.2. Crystal composition and structure

The crystal composition was examined by the energy dispersive X-ray (EDX) analysis. For each x value, 3~5 pieces of as-grown single crystal were selected from the crystals cleaved from different parts of the as-grown ingot and taken EDX measurement. One of the typical EDX spectrums for $x=0.40$ is shown in Fig.2. The crystal composition normalized to $\text{Sr}=1.60$ is $\text{Bi}_{2.41}\text{Sr}_{1.60}\text{Cu}_{1.05}\text{O}_{6.36}$. Note that the composition of oxygen is not precise as other elements because the EDX is not sensitive to light atoms. From the result, it can be seen that the crystal composition is close to the starting material and Cu has slightly more sufficient content than $\text{Cu}=1$. For other x values, the results are similar to $x=0.40$ except for $x=0.05$ and 0.04 because of the inhomogeneity of those needle-like crystals. However, there is no remarkable difference between crystals grown under $P(\text{O}_2)=2$ and 6 atm .

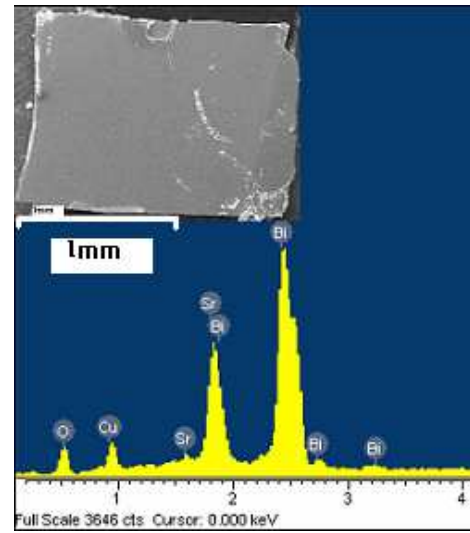


Fig. 2. (color online) Typical EDX spectrum for the single crystal with $x=0.40$, the inset is the SEM photo of this crystal. The crystal composition normalized to $\text{Sr}=1.60$ is $\text{Bi}_{2.41}\text{Sr}_{1.60}\text{Cu}_{1.05}\text{O}_{6.36}$.

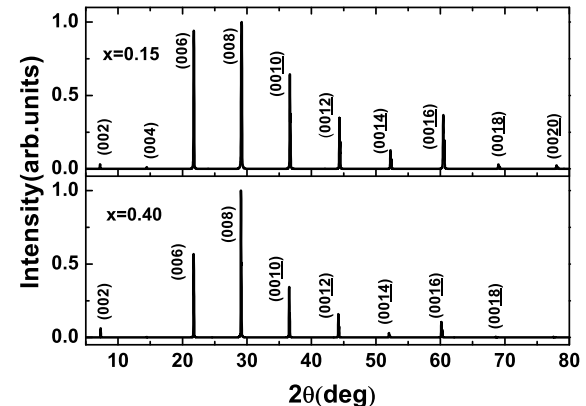


Fig. 3. XRD patterns for the single crystals with $x=0.15$ and 0.40 .

In order to examine the structure of our samples, XRD measurement was carried out. The typical single crystal XRD patterns are shown in Fig.3. Only sharp even peaks along to c -axis could be observed. The full-width-at-half-maximum(FWHM) of each peak is about 0.12° . The peaks are splitting at high degree angle due to different wavelength effects between $K_{\alpha 1}$ and $K_{\alpha 2}$ radiation. XRD for the polycrystal and starting material after premelting was also carried out before crystal growth, and comparing with the XRD patterns for the single crystal, it is found that the peaks from three sets of data coincide very well.

Figure.4(a) shows that the (006) peak moves with the varied x value. While Fig.4(b) shows the x value dependence of the c -axis lattice parameters for the single crystals grown under $P(\text{O}_2)=2$ atm. The values of c -axis parameters calculated from other peaks have a little difference, but the whole trend is similar to Fig.4(b). From Fig.4(b) we can see that when the x value increases, more and more Sr^{2+} are substituted by Bi^{3+} in the $\text{Sr}-\text{O}$ plane, the c -axis lattice parameter decreases rapidly starting from $x=0.25$, since the size of Bi^{3+} ($d=0.96$ Å) is smaller than Sr^{2+} ($d=1.12$ Å).

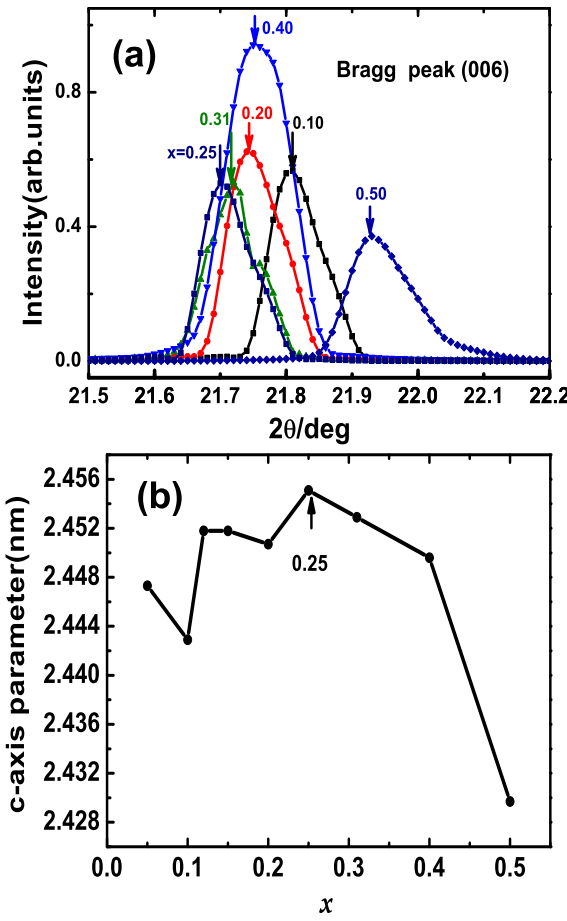


Fig. 4. (color online) (a). The (006) peaks with the varied x values. (b). The x value dependence of the c -axis lattice parameters for the single crystals grown under $P(O_2)=2$ atm.

Å). The c -axis is compressed slightly under the case with $P(O_2)=6$ atm, but the behavior of the c -axis parameters is similar to that shown in Fig.4(b).

3.3. Superconductivity

The AC susceptibility was measured on more than 20 pieces of crystals which were cleaved from different parts of the as-grown ingot for each x value. Fig.5 shows three typical curves of the AC susceptibility for $x=0.14$, 0.10 and 0.05 crystals, the T_c was defined as the point where the real part of the susceptibility becomes flat, namely, the onset point. The superconducting transition width ($\Delta T_c=T_c(90\%) - T_c(10\%)$) of the crystals is very sharp, about $0.5 \sim 1.3$ K. However, due to the strong anisotropy of bismuth based single crystals, it is almost impossible to obtain single-domain as-grown ingot[10,19,20]. Actually, the orientation of c -axis was always perpendicular to the growth direction. The cleaved surface was always ab -plane, so the thickness of cleaved crystals was always small. However, it was reported that higher pressure of oxygen lead to thicker and sizeable crystals[9,10]. But by using 6 atm oxygen pressure during the growth, the results

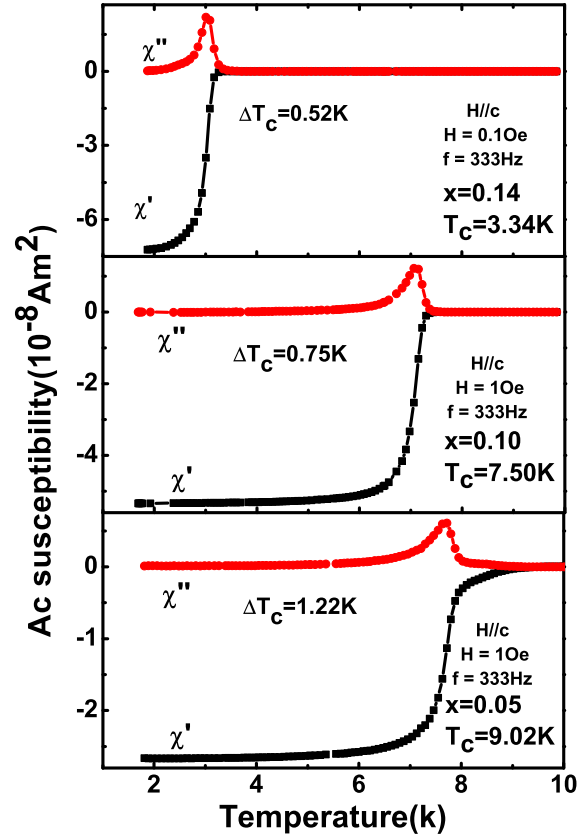


Fig. 5. (color online)AC susceptibility for $x=0.14$, 0.10 , 0.05 single crystals, the T_c was defined as the point where the real part χ' derates from the flat part, and $\Delta T_c=T_c(90\%) - T_c(10\%)$.

were not improved obviously, and the T_c was increased less than 0.5K compared with $P(O_2)=2$ atm. Actually, due to the random growth direction of crystals, the segregation always exists, this leads to the slightly difference of T_c of different pieces cleaved from the same ingot. The curves of the AC susceptibility for all crystals cleaved from the same ingot were drawn together, and the T_c for each x value was determined by statistic method, that is, the average value for samples with close T_c values.

As known for cuprate superconductors, post-annealing under different temperature and atmosphere could change the oxygen content, and thus the doping level as well as T_c . But it seems difficult to change the T_c of BSCO by annealing. The temperature was varied 20°C per step from 400 to 600°C when annealing was carried out in oxygen or nitrogen atmosphere for 100 hours each time. But the curves of the AC susceptibility for the same crystal moved a little after annealing, the largest change was less than 0.5K. So the T_c was derived from high quality as-grown single crystal for each x value.

Fig.6 shows the resistivity of as-grown single crystals, where Fig. 6(a) and Fig. 6(b) show the resistivity of the single crystals grown under 2atm and 6atm pressure of oxygen, respectively. All resistivity curves were normalized by $\rho(T=280 \text{ K})$ in order to compare with each other. From Fig.6 we can see that most of the curves show underdoped

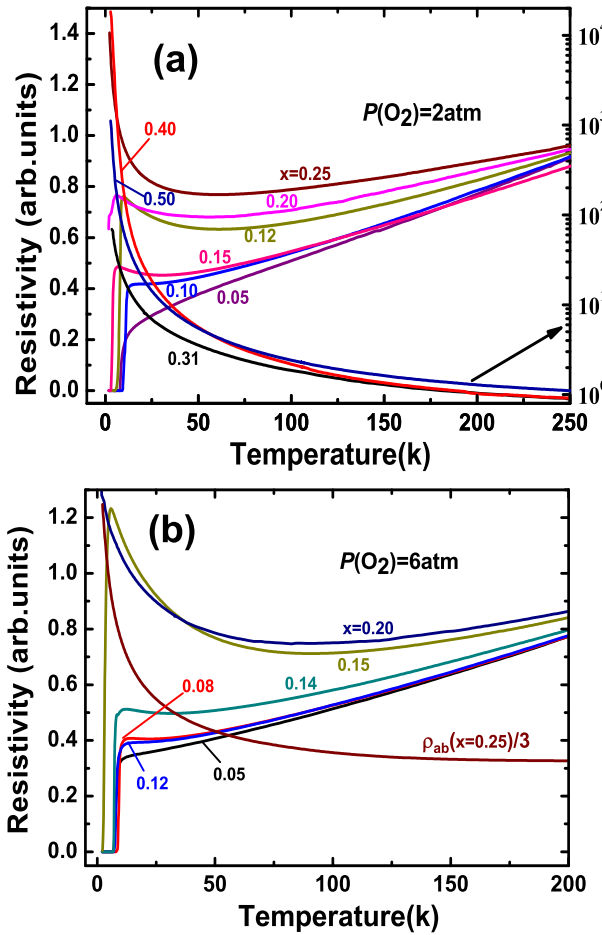


Fig. 6. (color online) Temperature dependence of resistivity for BSCO single crystal. Fig. 6 (a) and (b) show the resistivity of BSCO grown under oxygen pressure $P(O_2)=2$ atm and $P(O_2)=6$ atm, respectively. Where resistivity for the samples with $x=0.31, 0.40, 0.50$ was corresponding to the right axis with a logarithmic scale.

behavior, except for $x=0.05$ in Fig. 6(a), which shows over-doped feature. When the temperature is close to 0 K, the upturn of resistivity becomes more serious as x value increases. This effect is due to the localization of carriers which is induced by the out-of-plane disorder. The resistivity for $x=0.31, 0.40$ and 0.50 samples which correspond to the right axis in Fig. 6(a) become drastically divergent when T approaches 0 K. Moreover, the temperature dependence of the crystal resistivity under magnetic field up to 9T was measured recently. The negative magnetoresistance effect was observed in the weak localized region of resistivity, which may be explained by the localization effects.[21,22]

The evolution of T_c with varied x was shown in Fig. 7, the T_c values were derived by statistic method as illustrated above. It is known that the hole doping decreases as x value increases, thus the substitution of Sr^{2+} with Bi^{3+} enhances the electron doping and reduces the hole concentration. It is obvious that all samples with x varied from 0.05 to 0.50 were in underdoped region, this can be confirmed further by resistivity measurement. For the samples with $x=0.05$ which is close to optimal doping level, T_c varys in wider

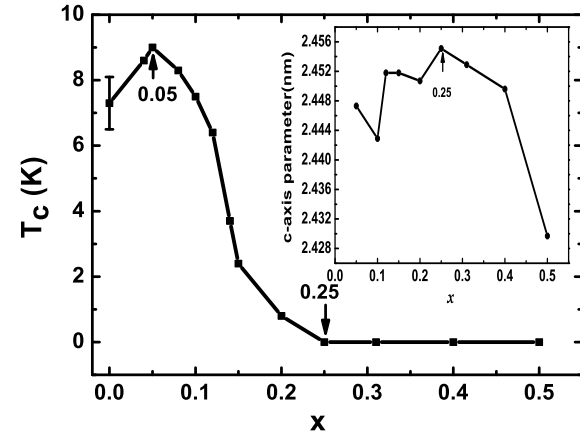


Fig. 7. The doping dependence of T_c of the as-grown BSCO single crystals. The inset shows the corresponding behavior of c-axis parameters.

range in different parts of the same ingot. And for the samples with $x=0.04$, the situation is similar to $x=0.05$, but most samples are overdoped. In addition, the T_c of samples with $x=0.20$ was derived by extrapolating the resistivity to zero at low temperatures, and for samples with $x \geq 0.25$, no superconductivity was observed down to 1.6K. Fig. 7 shows the relation of T_c vs. x and it seems that a hall dome shape emerges. The inset shows the corresponding behavior of c-axis parameters. It is interesting to note that there is a strong correlation between T_c and the c-axis parameters. The vanishing of superconductivity starts from the point where the contraction of c-axis occurs, which suggests that the superconductivity is strongly influenced by a subtle change of the structure.

4. Conclusions

High quality underdoped $Bi_{2+x}Sr_{2-x}CuO_{6+\delta}$ single crystals were successfully grown by TSFZ method. Higher pressure of oxygen during growth and post-annealing have little effects on the c-axis parameters and T_c . There is a strong correlation between the c-axis parameters and T_c suggesting a influence on superconductivity by a subtle change of the structure. The superconductivity vanishes at $x=0.25$, and the resistivity of crystals with $x \geq 0.31$ become drastically divergent with T down to zero showing a strong localization effect induced by the out-of-plane disorder.

5. Acknowledgement

This work is supported by the National Science Foundation of China, the Ministry of Science and Technology of China (973 project: 2006CB601000, 2006CB0L1002), the Knowledge Innovation Project of Chinese Academy of Sciences (ITSNEM).

References

- [1] C. Michel, M.Hervieu, M.M.Borel, A.Grandin, F.Deslandes, J.Provost and B.Raveau, Z.Phys. B **68**,421(1987);
- [2] L. F. Schneemeyer, R. B. van Dover, S. H. Glarum, S. A. Sunshine, R. M. Fleming, B. Batlogg, T. Siegrist, J. H. Marshall, J. V. Waszczak, L. W. Rupp, Nature **332**,422(1988);
- [3] G.Xiao, M.Z.Cieplak and C.L.Chien, Phys.Rev.B **68**, 11824 (1988);
- [4] R. M. Fleming, S.A.Sunshine, L.F.Schneemeyer, R.B.Van Dover, R.J.Cava, P.M.Marsh, J.V.Waszczak, S.H.Glarum S.M.Zahurak and F.J.DiSalvo, Physica C, **173** (1990)37;
- [5] K.Remschnig, J.M.Tarascon, R.Ramesh and G.W.Hull, Physcica C, **175** (1991)261;
- [6] J.I.Gorina, G.A.Kaljushnaia, V.I.Ktitorov, V.P.Martovitsky, V.V.Rodin, V.A.Stepanov and S.I.Vedeneev, Solid State Commun. **91**, 615(1994);
- [7] T.Niinae, Y.Ikeda, Y.Bando, M.Takano, Y.Kusano, J.Takada, Physcica C, **313** (1999)29;
- [8] M. Matsumoto, J. Shirafuji, K. Kitahama, S. Kawai, I. Shigaki and Y. Kawate, Physcica C, **185-189** (1991)455;
- [9] C. T. Lin, B. Liang, M. Freiberg, K. Peters and E. Schönherr , Physcica C, **341-348** (2000)541;
- [10] B. Liang, A. Maljuk and C. T. Lin, Physcica C, **361** (2001)156;
- [11] M.S.Osofsky, *et al.*, Phys.Rev.Lett **71**, 2315(1993);
- [12] S.I.Vedeneev, A. G. M. Jansen, E. Haanappel, P. Wyder, Phys.Rev.B **60**, 12467(1999);
- [13] F.Bouquet, L.Fruchter, I.Sfar, Z.Z.Li and H.Raffy, cond-mat/0512093(2006);
- [14] A. Kanigel *et al.*, Nature Physics **2**, 447(2006)Letters;
- [15] Hai-Hu Wen, Lei Shan, Xiao-Gang Wen, Yue Wang, Hong Gao, Zhi-Yong Liu, Fang Zhou, Jiwu Xiong, and Wenxin Ti, Phys. Rev. B **72**,134507(2005);
- [16] H. Eisaki, N. Kaneko, D. L. Feng, A. Damascelli, P. K. Mang, K. M. Shen, Z.-X. Shen, and M. Greven, Phys.Rev.B **69**, 064512(2004);
- [17] K. Fujita, T. Noda, K. M. Kojima, H. Eisaki, and S. Uchida, Phys. Rev. Lett. **95**, 097006(2005);
- [18] A. Sugimoto, S. Kashiwaya, H. Eisaki, H. Kashiwaya, H. Tsuchiura, Y. Tanaka, K. Fujita, and S. Uchida, Phys. Rev.B **74**, 094503(2006);
- [19] B.Liang and C.T.Lin, J.Crystal Growth, **267**(2004)510;
- [20] B.Liang and C.T.Lin, J.Crystal Growth, **237-239**(2004)756;
- [21] T.W.Jing, N.P.Ong, T.V.Ramakrishnan, J.M.Tarascon and K.Remschnig, Phys.Rev.Lett. **67**,761(1991);
- [22] P.A.Lee and T.V.Ramakrishnan, Rev.Nod.Phys. **57**, 287(1985);